S. Middelhoek

Static Reversal Processes in Thin Ni-Fe Films

Abstract: Magnetization reversal at an angle to the easy direction in Ni-Fe films was studied. The results, in contrast to the single-domain theory, show no coherent rotation, even for field directions in which the critical field for rotation is smaller than the critical field for wall motion. The actual reversal is initiated by rotation of the magnetization in bands formed in the film. New experimental studies show that the reversal is subsequently completed by wall motion. A qualitative discussion of the new observations and a review of previous work give a comprehensive picture of the static reversal processes in thin Ni-Fe films.

Introduction

Thin 80-20 Ni-Fe films evaporated in the presence of a magnetic field exhibit a uniaxial anisotropy with the easy axis of magnetization parallel to the field direction.[1] When a magnetic field is applied in the plane of such a film, in general the magnetization is turned out of the easy direction. The resulting stable magnetization direction θ ($\theta = 0°$ being the easy direction), is found by minimizing the sum of the anisotropy and the field energies with respect to θ ($\partial E/\partial\theta = 0$, $\partial^2 E/\partial\theta^2 > 0$). With low fields two stable directions are possible, whereas with larger fields only one direction is stable. When one assumes that the single-domain state of the film is conserved, an irreversible transition from one state to another may occur by rotation of the magnetization at fields for which $\partial^2 E/\partial\theta^2 = 0$ and $\partial E/\partial\theta = 0$. When one calculates the field H_r at which this irreversible rotation occurs as a function of the direction β of the field with respect to the easy direction, one obtains the well-known astroid-shaped critical curve for rotation:

$$(H_x)^{2/3} + (H_y)^{2/3} = (2K/M_s)^{2/3},$$

in which K is the anisotropy constant and M_s is the saturation magnetization.[2] The critical field for rotation in the easy direction is $H_k = 2K/M_s$. The directions of the magnetization just before (θ_1) and just after (θ_2) rotation can easily be obtained by drawing the tangents to this curve through the tip of the field vector $\mathbf{H}_r$, as is shown in Fig. 1a.[3]

It is well known that the reversal behavior of thin Ni-Fe films cannot be completely described by the above single-domain theory, since wall-motion reversal processes also occur. These wall motions usually take place at lower critical fields (H_w) than those for rotation (H_r), for field directions close to the easy axis. Measurements of the critical field for wall motion, H_w, as a function of the angle β between the magnetic field and the easy direction ($H_w = H_c$ for $\beta = 0$), yield the critical curve for wall motion as sketched in Fig. 1b. The theoretical critical curve for rotation and the experimental critical curve for wall motion intersect at a certain angle β_c, as shown in Fig. 1b.[4] The magnitude of β_c depends on the ratio H_c/H_k, which in turn depends on the evaporation parameters. For so-called inverted films,[5] in which $H_c > H_k$, one finds $\beta_c = 0°$. In accordance with the single-domain theory, uniform rotation is expected to occur in the range $\beta_c < \beta \leqq 90°$. However, previous investigations by Methfessel, Middelhoek and Thomas[4] showed that even in this range no uniform rotation occurs. The reversal process which really occurs is rather complicated. It consists of a rotation of the magnetization in narrow bands in the film, which are perpendicular to the magnetization just before this rotation begins at a field H_p slightly larger than H_r. The process is called *partial rotation*[4] or *labyrinth switching*[6] and the explanations given are based on the dispersion of the anisotropy in Ni-Fe films. In the present work we will discuss the partial rotation process in more satisfactory detail, utilizing Bitter patterns and the Kerr magneto-optic effect.

As the range of field directions in which these partial rotation processes occur depends on the ratio between the critical field for wall motion (H_c) and rotation (H_k) in the easy direction, the discussion of the partial rotation process is preceded by a section which reviews the factors that are known to determine the magnitude

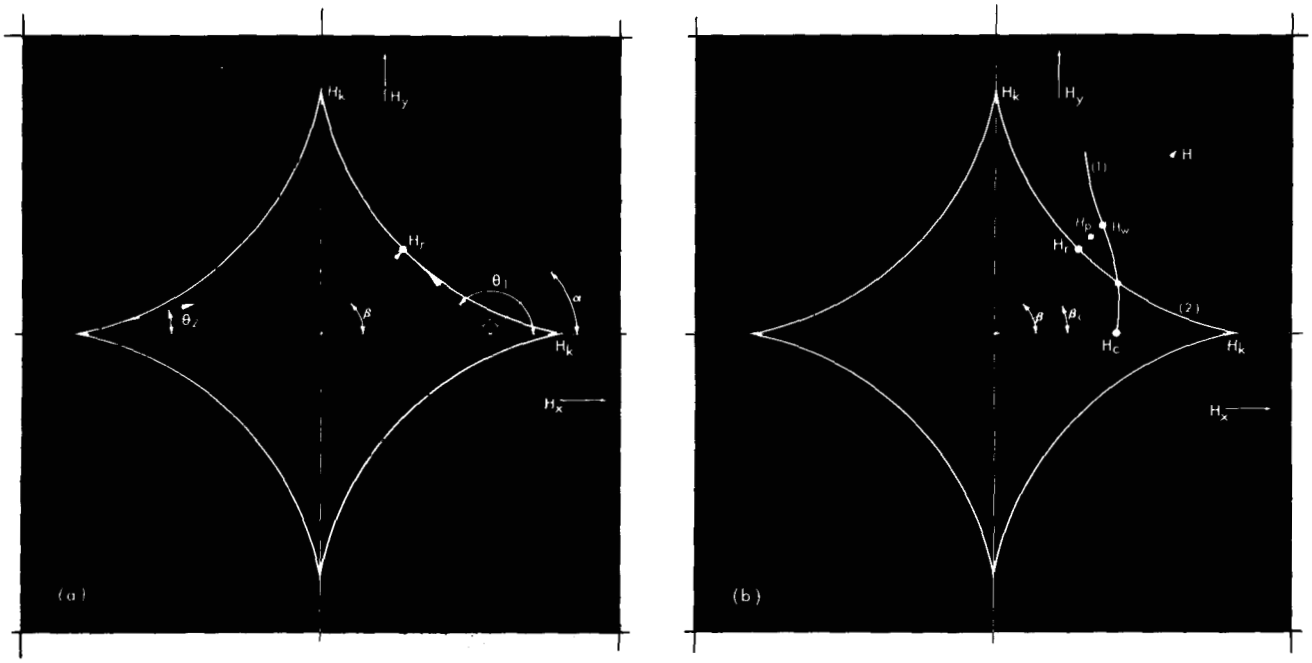

Figure 1 **(a) Theoretical critical curve for reversal by rotation.**

The magnetization directions just before (θ_1) and just after (θ_2) rotation are obtained by drawing the tangents to the curve through the tip of the field vector $\mathbf{H}_r$. β is the angle between the magnetic field and the easy direction.

(b) Critical curves for wall motion (1) and rotation (2).

The critical field for wall motion H_w in the easy direction is called H_c, whereas the critical field for rotation H_r in the easy direction is called H_k. For $\beta < \beta_c$ reversal occurs by wall motion, whereas for $\beta > \beta_c$ reversal takes place by partial rotation, followed by wall motion.

of the critical field for wall motion.

In the third section of this paper is described how the reversal is completed after partial rotation has taken place. Bitter patterns show that the reversal is actually completed by two different types of wall motion.

The final section deals with demagnetization processes as they occur when the field is switched off and reversed before the wall-motion processes start to complete the film reversal.

Wall motion

Thin Ni-Fe films, when subjected to a magnetic field with direction $0° < \beta \leqq \beta_c$, reverse their magnetization by domain wall motion. This wall motion starts from nuclei of reversed magnetization at the edges of the film, as is shown by the Bitter patterns of Fig. 2. As the applied field increases, these nuclei grow over the whole film, forming long walls parallel to the easy direction, and the reversal is completed by a parallel shift of these walls. Still very little is known about the origin of the wall-motion coercive force of thin films.

Néel[7] proposed a coercive force theory, which is based on thickness variations of the film. The result of this theory is the well-known 4/3 law, $H_c = C \cdot D^{-4/3}$, in which C is a constant and D the film thickness. The law is valid only for thick films, where Bloch walls occur; for Néel walls in thin films, the coercive force for wall motion is independent of the film thickness D, as is shown by the author elsewhere.[8] Behringer and Smith[9] showed that the 4/3 law still retains its validity for thick films, when the change of the magnetization direction in the wall is approximated by a function which allows a more precise calculation of the magnetostatic energy of the wall than the model on which Néel based his calculations.[10]

Encouraged by the work of Néel, a number of authors[11-18] have investigated the thickness dependence of the coercive force experimentally, but only in a single case was a reasonable agreement with the theory found.[11]

From the fact that the critical field for wall motion also depends strongly on the composition of the film[16,19] and is a minimum for those alloys for which the crystal anisotropy constant K_1 and the magnetostriction λ are small, it is obvious that the H_c-mechanism proposed by Néel cannot be the only one. Since crystalline and magnetostrictive anisotropies lead to a dispersion of the magnitude and the direction of the uniaxial anisotropy, it does not seem unreasonable to connect the coercive force for wall motion with this dispersion. Since the magnitude of the dispersion of the anisotropy

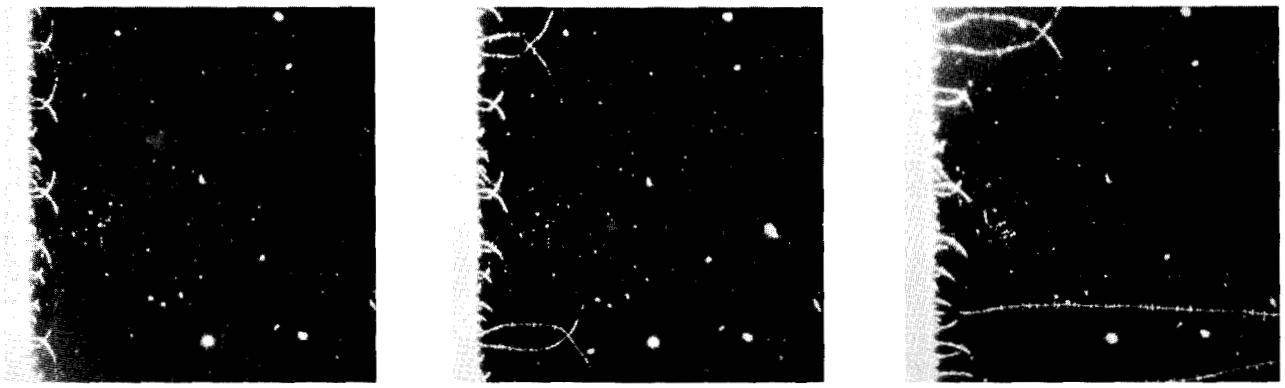

Figure 2 **Growth of nuclei having reversed magnetization at the edge of the film with increasing field.** *The field increases to the right.*

depends on the ratio of the stray anisotropies* to the uniaxial anisotropy, one may expect that the dispersion, and therefore also the wall-motion coercive force, will decrease when the uniaxial anisotropy is increased. This effect has been experimentally demonstrated.[20]

In summary, it seems plausible that the wall-motion critical field is mainly due to (a) film thickness variations and (b) dispersion of the anisotropy. Because of the incomplete understanding of the origin of the coercive force, it is still difficult to control the evaporation parameters to produce films with desired H_c/H_k ratio and β_c. In order to obtain films for which the critical angle β_c is small, those methods are used which, according to our experience, increase H_c or decrease H_k. Some of the methods are:

- The use of Fe-poor alloys,[21] which gives an increase of H_c and usually a decrease of H_k.[22]
- Evaporation at relatively high substrate temperatures ($200°C < T < 400°C$), which gives low H_k values. For very high temperatures ($T > 400°C$) H_k increases again.[23]
- Use of rough substrates, which increases H_c.
- Choice of that film thickness for which H_c is a maximum[14] ($D = 750$ A).

The films on which the observations in this paper were made were obtained by a combination of the above methods. A small angle β_c is necessary to insure that in a large range of field directions the partial rotation processes can be studied and compared.

Partial rotation

According to the single-domain theory, uniform rotation is expected to occur in the range $\beta_c < \beta \leqq 90°$. Magneto-optic Kerr observations (Fig. 3) show, however, that for all films in the range $\beta_c < \beta \leqq 90°$ at a field slightly larger than the theoretical critical field for rotation H_r in the respective direction, the film splits up into elongated domains. In the Kerr picture, the elongated domains appear dark and the area between the domains remains light, indicating that only in the elongated domains is the magnetization reversed to the new stable direction. Except for an area close to the edges, the domains suddenly appear, indicating that they are generated by a rotation process rather than by wall motion. For this film $\beta_c = 10°$ and reversal for $\beta = 0°$ to $10°$ occurs by wall motion.

The occurrence of partial rotation is caused by the dispersion of the direction and magnitude of the anisotropy, which in turn leads to a dispersion of the magnetization directions in the film. Variations in the local magnetization direction parallel to the direction of net magnetization (longitudinal ripple) give rise to a lower stray-field energy than that due to variations along a direction perpendicular to the net magnetization (lateral ripple). The magnetization, therefore, responds preferentially to those anisotropy variations which lead to longitudinal ripple.[24] This ripple consists of bands of equal deviation from the direction of net magnetization, which lie perpendicular to this direction (Fig. 4a). The ripple was shown clearly by Fuller and Hale[24] and later by Fuchs[25] by an electron-optical method. When the magnetization is turned out of the easy direction under the influence of an external magnetic field, the direction of the ripple turns also and remains perpendicular to the direction of the net magnetization (Fig. 4b). This change of orientation of the ripple with increasing field has been shown experimentally by Feldtkeller.[26] When the field is further increased, the critical field for rotation, H_r, of some of the bands is exceeded and the magnetization in these bands rotate to the other stable direction. This partial rotation causes the boundaries between the alternate bands to become real domain walls for

* We define the combination of crystalline and magnetostrictive anisotropies as the *stray anisotropies*.

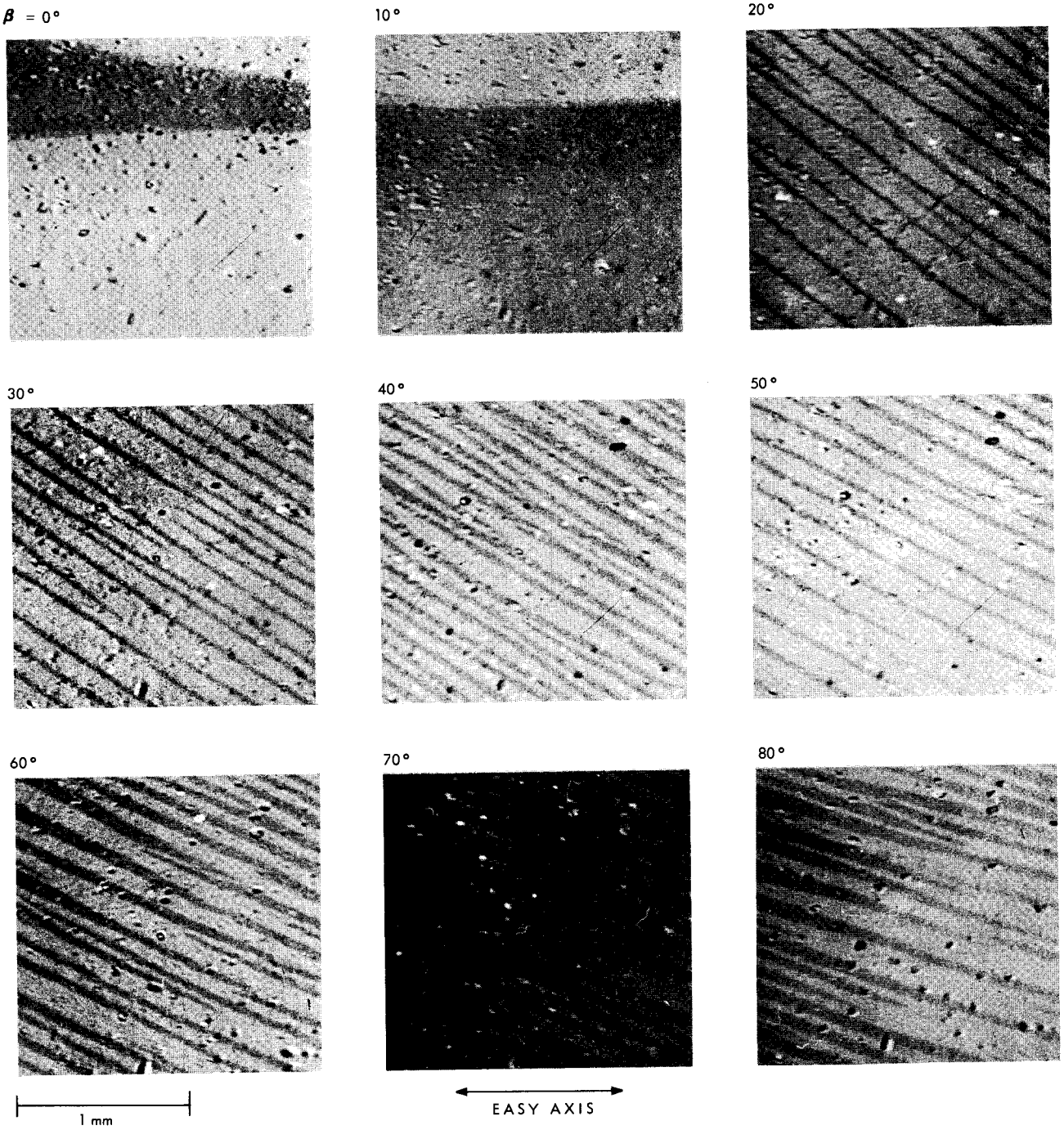

Figure 3 **Kerr magneto-optic observations of static reversal processes as a function of the angle β between the field and the easy direction.**

The pictures were taken for fields slightly larger than the critical fields for uniform rotation in the respective directions. For $\beta \leqq 10°$ wall motion occurs, whereas for $\beta > 10°$ partial rotation occurs instead of uniform rotation as expected on the basis of the single domain theory ($H_c = 4.1$ oe, $H_k = 6.0$ oe and $D = 460$ A). Here and in all following pictures the easy axis is horizontal.

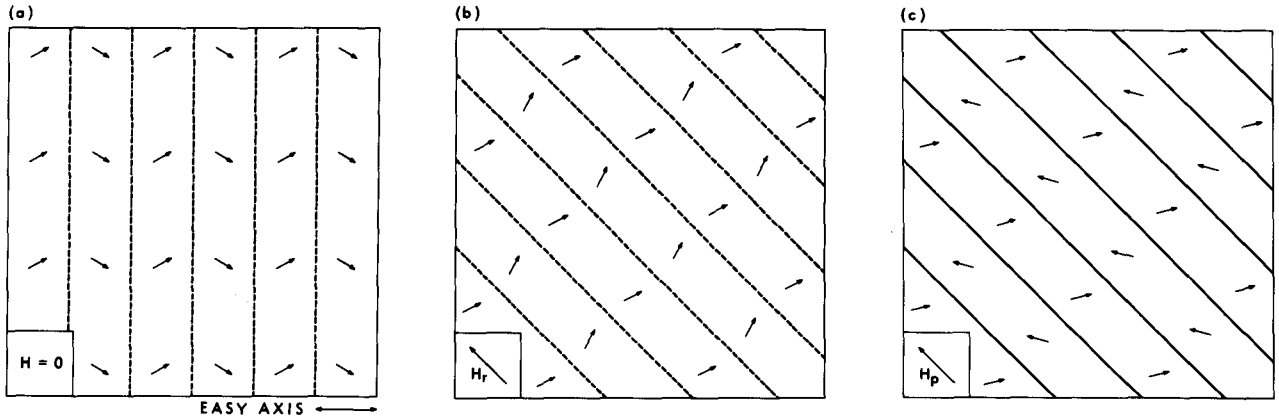

Figure 4 **(a) Schematic representation of the ripple pattern at zero field.** *The magnetization responds preferentially to those anisotropy variations which lead to longitudinal ripple.* **(b) Under influence of an external field the magnetization and the ripple pattern turn, such that the bands remain perpendicular to the direction of the net magnetization. (c) Domain structure after the occurrence of partial rotation.** *The ripple pattern which exists before partial rotation starts is further delineated by domain walls following partial rotation.*

which, however, the magnetization component normal to the wall is not continuous (Fig. 4c). This discontinuity results in large stray fields, which prevent the magnetization in the other bands from rotating, even at fields much larger than their critical fields. The angle α between the bands and the easy direction is determined by the ripple configuration just before rotation begins in a number of the bands. This direction is perpendicular to the tangent to the critical curve through the tip of the field vector $\mathbf{H}_r$ (Fig. 1a). For the angle θ_1 between the tangent and the easy direction, we have

$$\tan\theta_1 = dH_y/dH_x = -(H_y/H_x)^{1/3},$$

and as $\tan\beta = H_y/H_x$, we obtain $\tan\theta_1 = -(\tan\beta)^{1/3}$.

The long domains are perpendicular to the tangent such that we obtain, for the angle α between the domains and the easy direction,[27] $\tan\alpha = (\tan\beta)^{-1/3}$.

In Fig. 5 this theoretical dependence is plotted together with the experimental dependence as obtained from Fig. 3. Both curves are in good qualitative agreement, although the measured angles are smaller than the ones predicted theoretically. For field angle β in the range of 0° to 10°, no measuring points are obtained, because here wall motion occurs.

Similar results were obtained by Smith and Harte[28] but their explanation is based on a different model of magnetization reversal. Smith and Harte showed that the deviation of the experimental curve from the theoretical is larger for a very thin film than for a thick film. For a number of films with different thicknesses the angle α between the domains and the easy axis was measured by the author. The measurement was done for an angle β of 60° between the field and the easy axis, as for nearly all films $\beta_c < 60°$. For this angle the theoretically expected value for α is 40°. The results are plotted in Fig. 6. For very thick films the agreement between theory and experiment is indeed very good.

Figure 5 **The angle α between the elongated domains, originated by the partial rotation process, and the easy direction as a function of the field angle β, as predicted by theory and obtained from Figure. 3.**
Since $\beta_c = 10°$, for $\beta = 0°$ to 10°, no measurements are obtained.

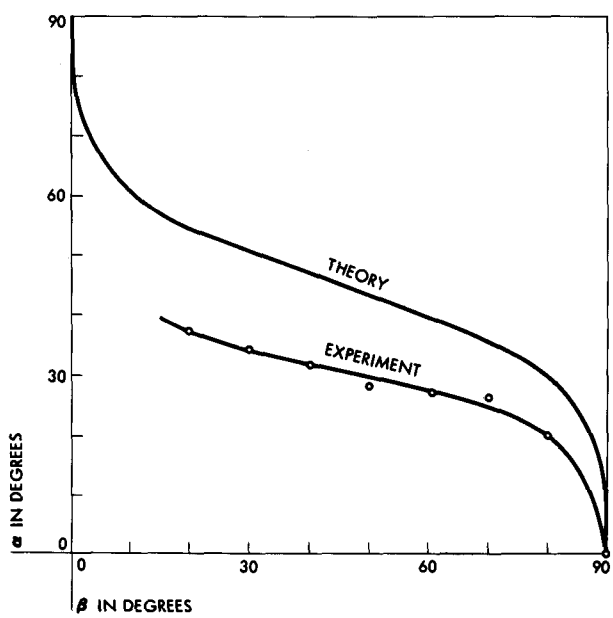

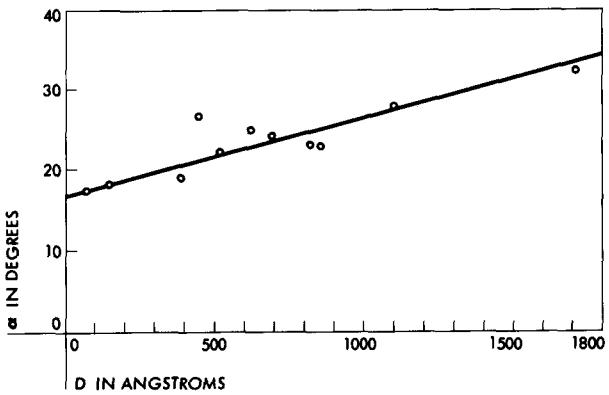

Figure 6 **The angle α between the elongated domains and the easy direction as a function of the film thickness D.**
Measurements were performed for $\beta = 60°$, as for practically all films $\beta_c < 60°$. For $\beta = 60°$ the theoretically expected value for α is 40°.

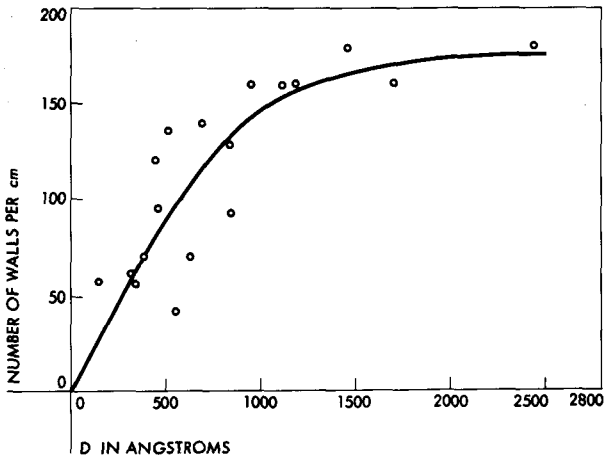

Figure 7 **Wall density N as a result of partial rotation as a function of the film thickness; again the measurements were performed for $\beta = 60°$.**

Furthermore, the Kerr and Bitter observations indicate that there is a relation between the fineness of the splitting-up pattern and the thickness of the film. The results obtained on a great number of films, all with H_c and H_k values in the range of 2 to 5 oe, are shown in Fig. 7. The wall density N increases for increasing thickness.

Partial rotation results from the existence of anisotropy dispersion in the film. Without the long-range effect of the stray-field coupling, however, each small region of the film would switch independently as its own anisotropy field is exceeded. That this does not in fact occur is due to the stray-field coupling between the different regions. When the regions with the lower anisotropy fields are switched, the regions with the higher anisotropy fields can no longer switch at their own anisotropy fields. In this region the stray field due to the noncontinuity of the magnetization component normal to the wall between the switched and nonswitched bands must also be overcome. The stray-field coupling becomes smaller as the film thickness decreases. While the mechanism is not fully understood, the experiments indicate that in thin films a readjustment of the wavelength and average direction of the ripple occurs before the stray-field coupling is sufficient to produce bands in which the rotational process is prohibited by the stray field.

The long domains need not all appear at the same field strength, as shown in Fig. 8. The fact that the later domains have the same width as the others, and are exactly in-between the others, indicates very strongly that the band structure is already determined before the partial rotation process starts.

The general question arises as to why such a band structure with its high stray-field energy does not change to a state with a lower stray-field energy, as Prutton[29] assumed. This means however, that the walls separating the differently magnetized domains have to turn and to move such that the magnetization component normal to the wall becomes continuous. According to our interpretation, the energy of these walls is very high because of an extra stray-field energy, which results from the discontinuity of the magnetization component normal to the wall. Therefore the coercive force of these walls will also be high, and reorientation at fields of the order of H_r cannot take place.

Complementary reversal processes

The partial rotation process, as shown in Fig. 3, leaves the film in a partially reversed state, and the question arises as to how the film reversal is completed when the field is increased. These processes were investigated by means of the Kerr and the Bitter techniques, and the results indicate that the nature of the complementary reversal processes also depends on the angle β between the field and the easy axis.

As is shown theoretically by Thomas[30] a rather large field is necessary to overcome the stray field which prohibits the rotation in the remaining bands. When β is just larger than β_c one can see from Fig. 1b, that the critical field for wall motion H_w just exceeds the critical field for rotation H_r. Observations show that in this field direction the partial rotation is followed by the motion of walls, which are nucleated at the edges of the film, just as is observed for $0° \leqq \beta < \beta_c$. Such a complementary wall motion process is shown in Fig. 9. The walls are usually roughly parallel to the easy direction. For large β, however, the walls nucleated at the edges tend to become normal to the walls which separate the reversed from the nonreversed bands, as is shown in the Kerr picture of Fig. 10.

The question arises as to whether the reversal can be completed by a motion of the walls separating the reversed from the nonreversed bands. The discontinuity of the magnetization component normal to these walls is very large, especially for small β, and leads to an additional stray-field energy term in the wall energy. The coercive force of these walls therefore will be also very high, so that completion of the reversal is performed by the easier moving walls generated at the edges of the film. For large angles β, the direction of the walls between the reversed and nonreversed bands is more nearly parallel to the easy axis, as can be seen in Fig. 3. The extra stray-field energy of the walls is then smaller and thus makes possible the completion of the flux reversal by the motion of these walls. The above discussion is confirmed by the results shown in Fig. 11, which are the Bitter patterns of a film switched by a field making an angle of 60° with the easy axis. For intermediate β both processes occur simultaneously. In Fig. 12 the different complementary

Figure 8 **Subsequent partial rotation of different parts of the film on slightly increasing the field from (a) 3.25 oe to (b) 3.40 oe.** *The later bands have the same width as the others and are exactly in-between the others. This strongly indicates that the band structure is already determined before partial rotation begins. (Same film as Fig. 3, $\beta = 60°$).*

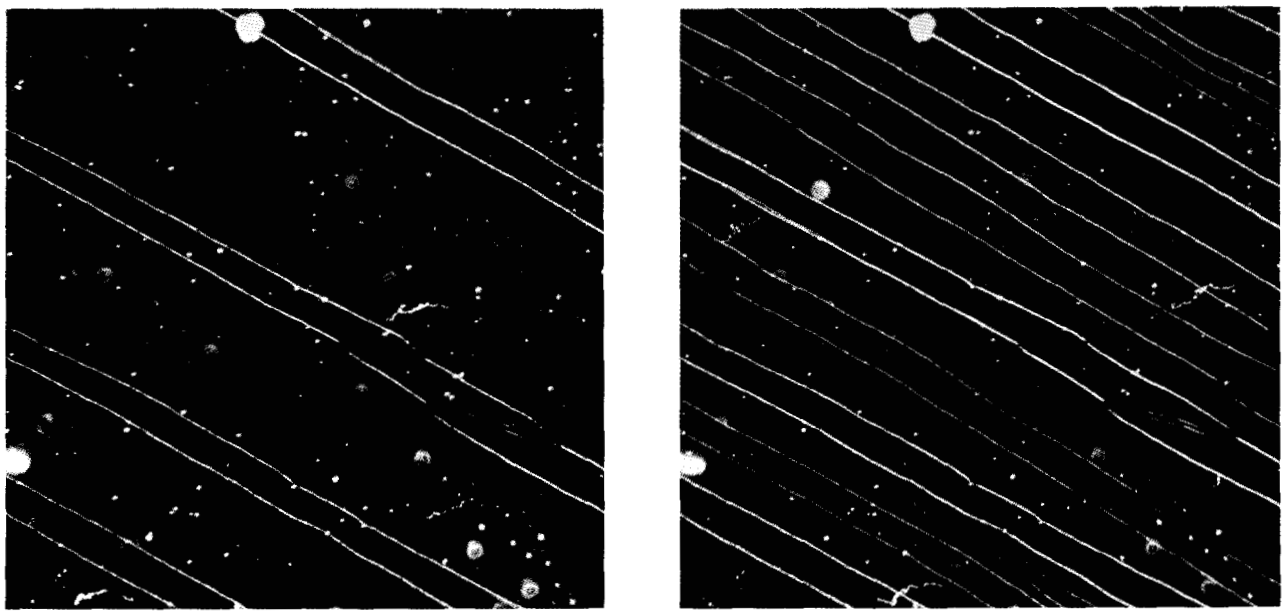

Figure 9 **Partial rotation followed by the motion of the walls nucleated at the edges of the film.** *The walls tend to be roughly parallel to the easy axis. (Same film as Fig. 3, $\beta = 30°$, (a) $H = 3.42$ oe, (b) $H = 3.83$ oe and (c) $H = 4.08$ oe.)*

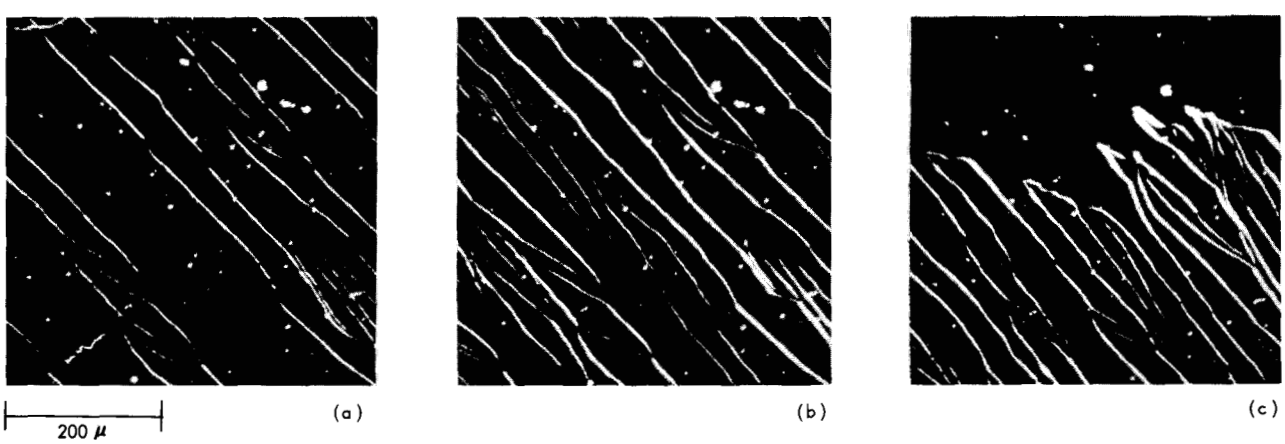

reversal processes are indicated, together with the critical curve (for experimental reasons measurement for $\beta > 85°$ was not possible). The critical curve is drawn using the H_k value as obtained from the slope of the hard direction hysteresis loop for small-field amplitude. The film was brought into a single-domain state by a large magnetic field just before the measurement of the slope. The possible error in the measurement is indicated by two dashed lines at both sides of the critical curve. For $0° \leqq \beta \leqq 10°$ reversal takes place by wall motion at fields lower than H_r. For $\beta > 10°$ partial rotation occurs at fields slightly larger than H_r, and the reversal is completed by the motion of the walls nucleated at the edges. For even larger β the motion of the walls surrounding the nonreversed bands also occurs; in fact, this is the only complementary reversal process for $\beta > 55°$.

The distinction between the different processes in rather thick films is no problem; in very thin films ($D \approx 100$ A), however, the distinction is not as easy. It is demonstrated by the Kerr pictures in Fig. 13, where wall motions (a) and partial rotation processes (b) are shown.

Figure 10 **Partial rotation followed by wall motion.**
The walls show a tendency to become perpendicular to the elongated domains. The easy axis is horizontal. ($H_c = 3.1$ oe, $H_k = 2.8$ oe, $D = 700$ A, $\beta = 30°$ and the applied field $H = 2.5$ oe).

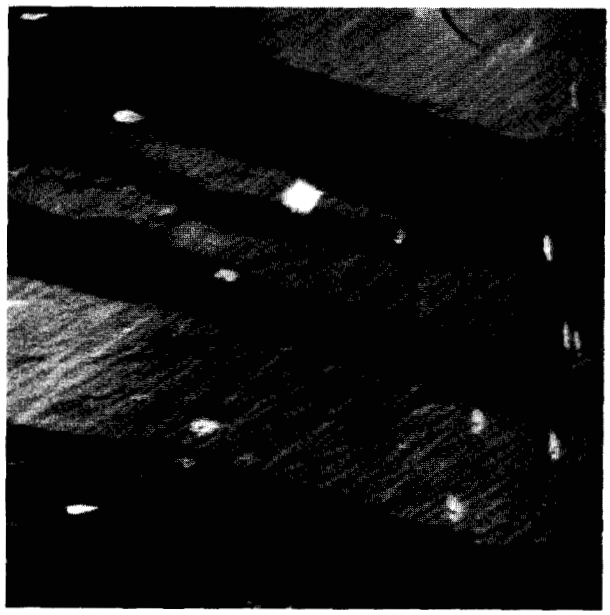

1 mm

Demagnetization processes

As already mentioned, the domain configurations which arise from the partial rotation process are associated with a high magnetostatic stray-field energy. This stray-field energy is a result of the fact that the walls which separate the reversed from the nonreversed bands have such a direction that the normal component of the magnetization is no longer continuous. When the external field is reduced before wall motion processes can occur, the bands with reversed magnetization will demagnetize. As can be seen from the Bitter patterns of Fig. 14b, and also as shown by Feldtkeller by the electron-optical method,[26] the bands demagnetize by splitting up in a great number of alternately magnetized domains.[4] When an additional small field in the reverse direction is applied, this demagnetization splitting is more accentuated (Fig. 14c). Smith and Harte[28] have assumed that the "labyrinth" shape of the bands is inherent to the reversal process itself. As shown here, however, the unusual shape of the domains is actually due to a demagnetization of the bands. From a magnification of the bands just before and just after demagnetization occurs (Fig. 15) it can be seen that the demagnetization takes place by a kind of buckling.[31] The place where a reverse domain will appear is

Figure 11 **Partial rotation, followed by motion of the walls, which separate the reversed from the nonreversed bands.** *(Same film as Fig. 3, $\beta = 60°$ (a) $H = 3.75$ oe, (b) $H = 4.33$ oe and (c) $H = 5.00$ oe.)*

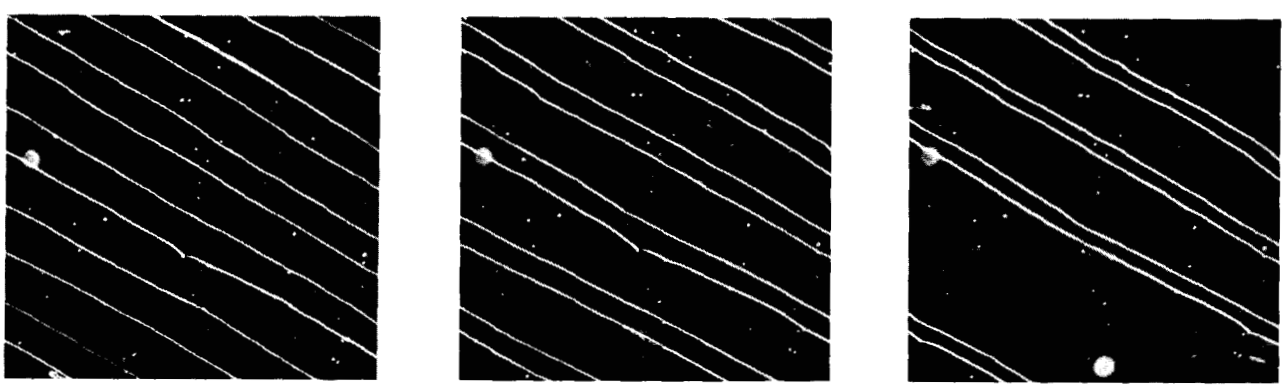

200 μ

(a) (b) (c)

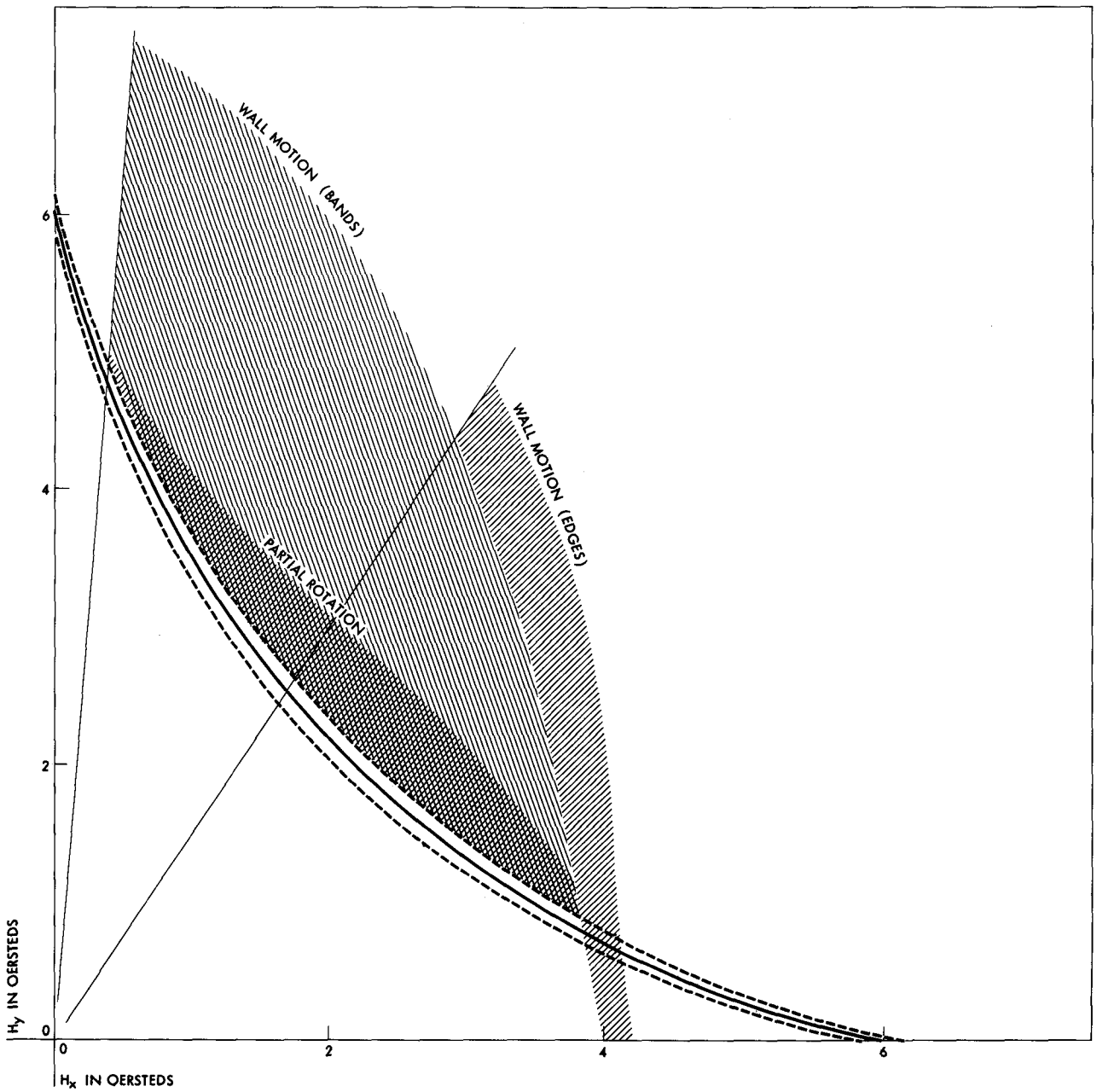

Figure 12 **Schematic representation of the different static reversal processes observed in the film of Figure 3.**

The critical curve is drawn using the H_k value as obtained from the slope of the hard-direction hysteresis loop for small field amplitude. The dashed lines indicate the maximum measurement error. The reversal processes can be divided into three ranges:

$0° \leqq \beta \leqq 10°$ *Motion of walls mainly nucleated at the edge of the film.*

$10° < \beta < 55°$ *Partial rotation, followed by motion of the walls separating the reversed from the nonreversed bands, finally followed by the motion of the walls nucleated at the edges.*

$55° < \beta < 90°$ *Partial rotation, now only followed by motion of the walls between the bands.*

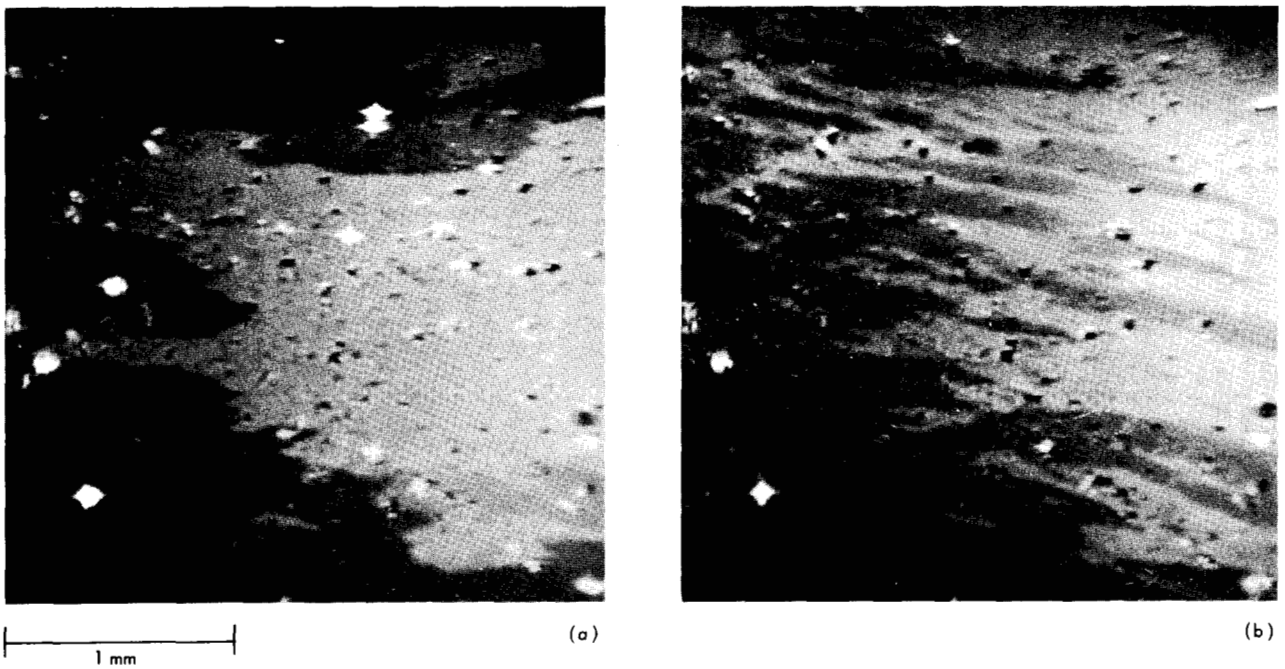

Figure 13 **(a) Wall motion ($\beta = 10°$, $H = 1.9$ oe) and (b) partial rotation ($\beta = 70°$, $H = 2.8$ oe) in a very thin film ($H_c = 2.0$ oe, $H_k = 4.0$ oe and $D = 120$ A).**

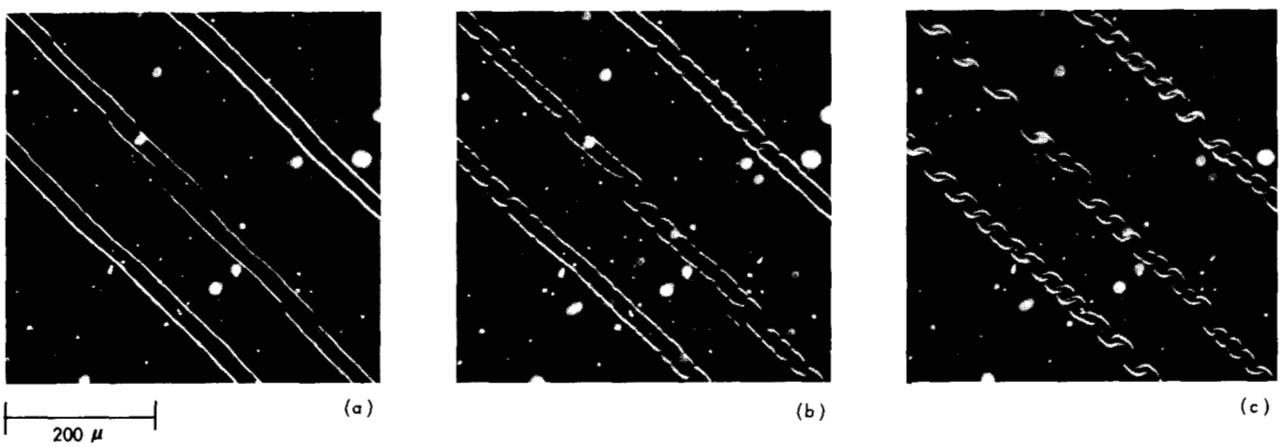

Figure 14 **Demagnetization of the reversed bands.**
Labyrinth shape appears after switching off the external field. A field in opposite direction accentuates the demagnetization pattern. (Same film as Fig. 3, $\beta = 20°$ (a) $H = +4.0$ oe, (b) $H = 0.0$ oe and (c) $H = -1.0$ oe.)

marked by small interruptions in the walls, suggesting magnetization distributions as drawn in Fig. 16.

Another interesting effect is that in all cases demagnetization occurs in the bands in which the magnetization is already reversed and not in the other bands. For reasons of symmetry, at first there would appear to be no preference for one kind of the bands, especially when all are of the same width. The reason for this preferential demagnetization of the reversed bands can be found in the direction of the magnetization in the Néel walls which separate the bands. As shown in Fig. 17, the magnetization direction in the wall is defined by the magnetization direction in the film just before partial rotation occurs. These Néel walls now cause a stray field which, in one pair of the domains must be added to, and in the other pair must be subtracted from the stray field because of the discontinuity of the magnetization component normal to the wall. The stray field becomes largest in the domains in which the magnetization is already reversed and that explains why these domains preferably demagnetize.

When the angle β between the field and the easy

direction is large, the domains after partial rotation are almost parallel to the easy direction and the stray field due to the discontinuity of the magnetization component normal to the wall is small. Bitter observations show that no demagnetization occurs and that at zero field the domain configuration is the same as that formed by partial rotation. On the application of a reverse field, at a certain field strength, the visibility of parts of the wall suddenly decreases, as is shown in Fig. 18. This sudden decrease in visibility is explained with the help of Fig. 19. In zero field the magnetization is in the easy direction and the bands are separated by

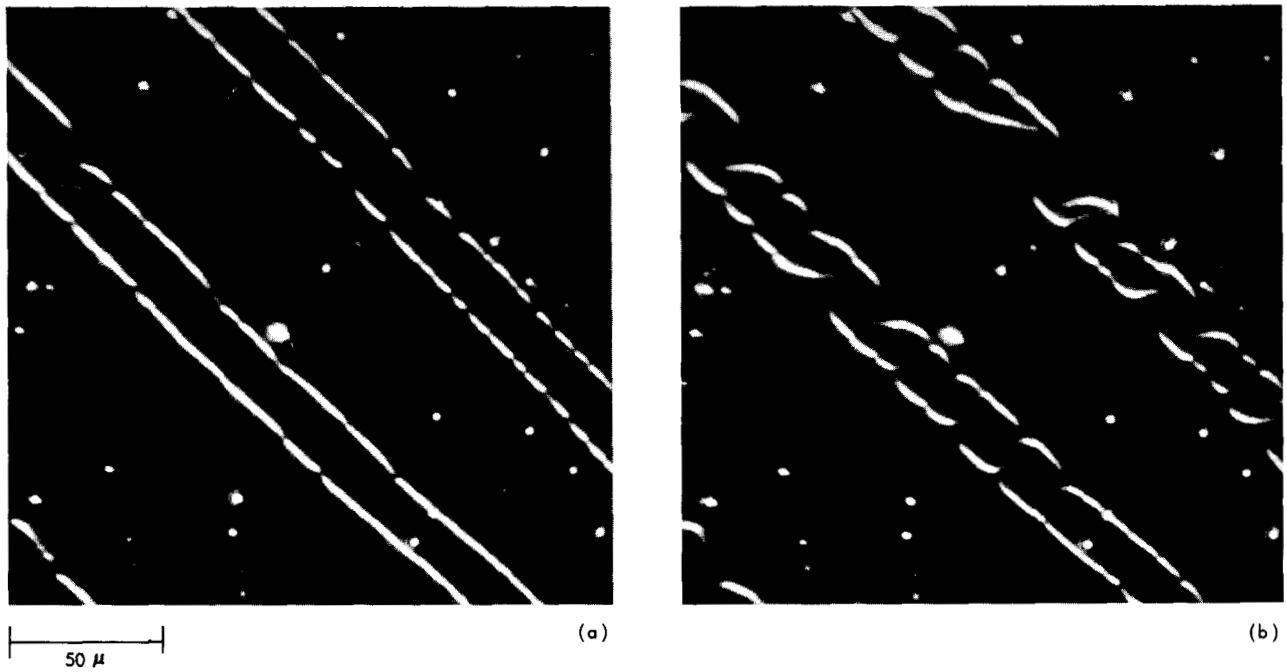

Figure 15 **Magnification of demagnetization process.** *The appearance of the reverse domains is preceded by a break-up of the domain walls. (Same film as Fig. 3, $\beta = 30°$ (a) $H = 0.0$ oe and (b) $H = -1.5$ oe.)*

Figure 16 **Schematic drawing of the buckling process during demagnetization of the bands (a) no external field and (b) negative external field.**

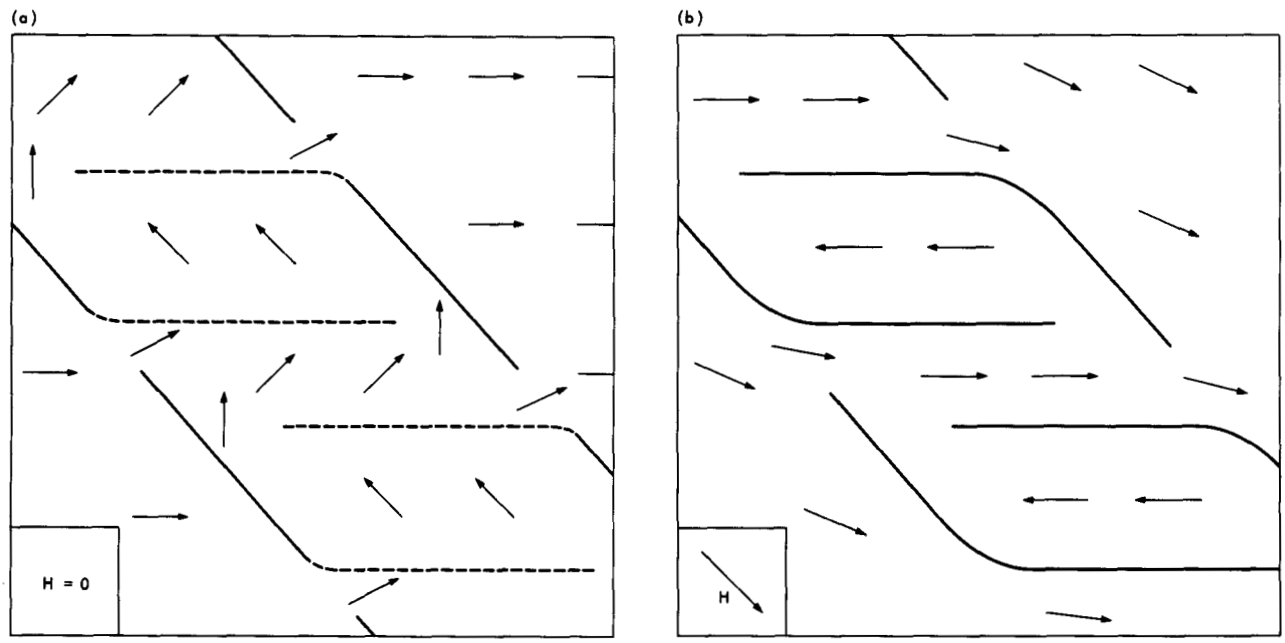

nearly 180° Néel walls. Increasing the reverse field forces the magnetization in the bands to turn in such a way that the angle through which the magnetization turns in the wall increases beyond 180°. At a certain field strength the angle between the magnetization directions in the neighboring domains is $\delta°$, and thus permits either $\delta°$ or $(360 - \delta)°$ walls. However, only $(360 - \delta)°$ walls exist and they have a much higher energy.[3,2] Consequently transition from the $(360 - \delta)°$ wall, having high magnetic pole density at the surface, to the $\delta°$ wall with low magnetic pole density should and does occur, resulting in a decrease

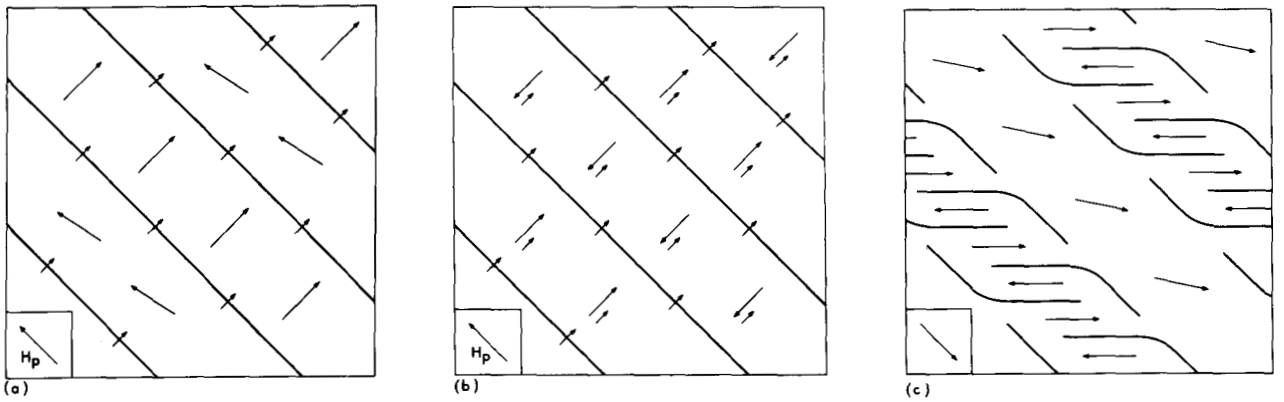

Figure 17 **Schematic drawing of the demagnetization process, showing that in the reversed bands the stray field is the highest, as there the stray field due to the discontinuity of the magnetization component normal to the wall and the stray field due to the Néel walls are to be added.** *(a) Magnetization distribution, (b) stray-field distribution and (c) final demagnetization configuration.*

Figure 18 **Bitter patterns of the reversal process as it occurs when the angle β between the field and the easy axis is large.** *Visibility decrease of the walls indicates that transitions from large angle to small angle Néel walls have occurred. (Same film as Fig. 3, $\beta = 60°$ (a) $H = -3.42$ oe and (b) $H = -3.67$ oe.)*

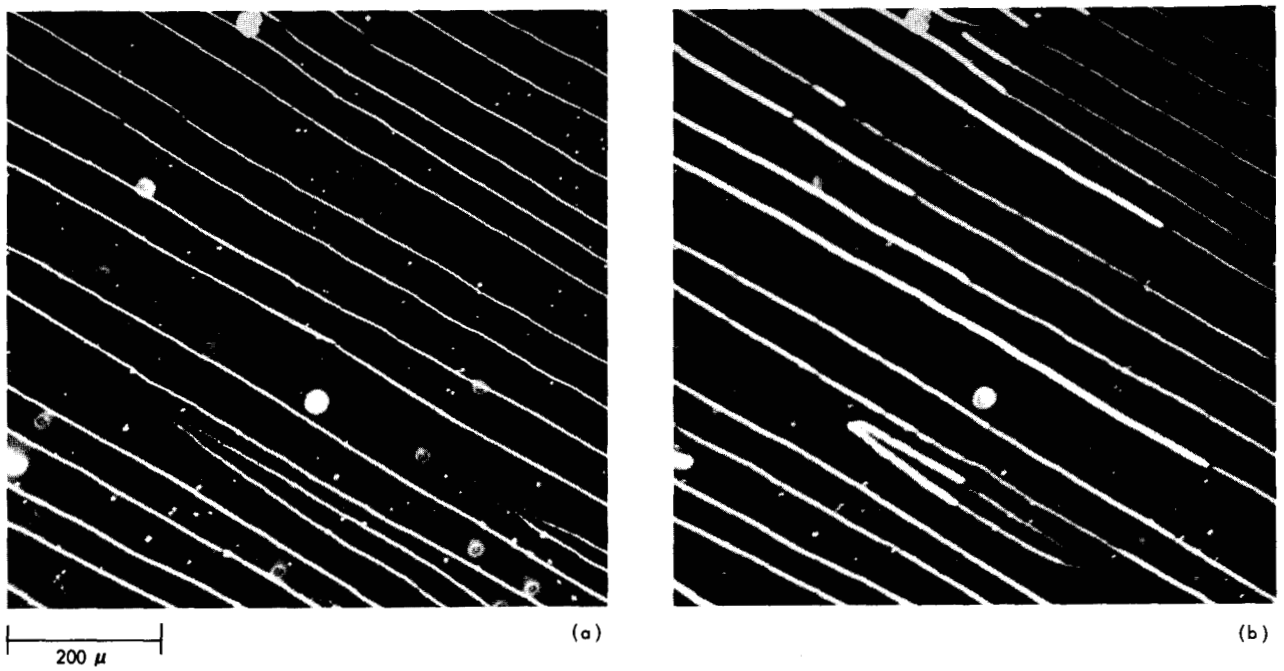

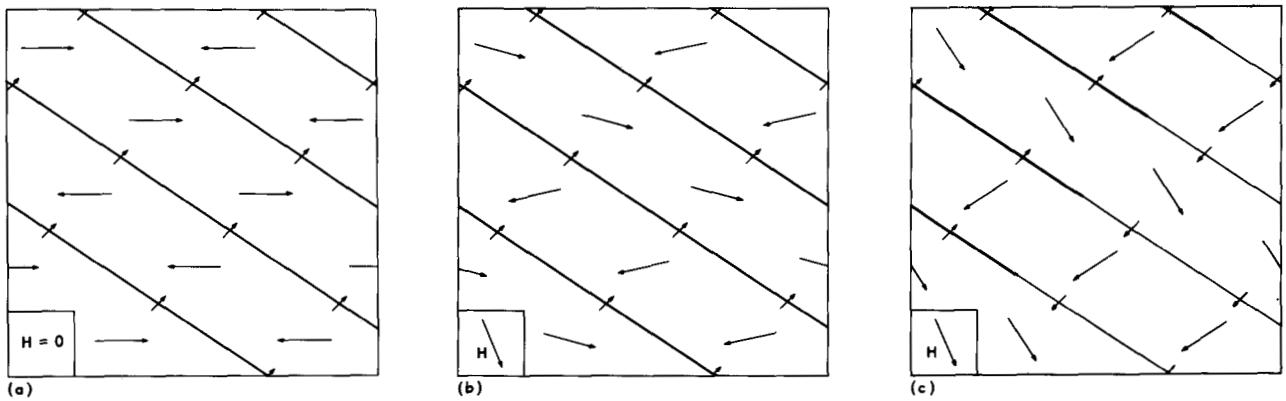

Figure 19 **Magnetization distribution for Figure 18.** *(a) No external field (b) small negative field and (c) large negative field causing a transition from large-angle to small-angle Néel walls.*

of visibility of the Bitter pattern. Probably this transition occurs by the shift of a Bloch line[33] along the wall, separating the $(360 - \delta)°$ and the $\delta°$ walls. A further increase of the magnetic field causes the walls themselves to move in the manner shown in Fig. 11.

Conclusions

Kerr effect and Bitter technique observations are discussed, showing that the static reversal processes deviate from those predicted by the single-domain theory. For small angles between the field and the easy axis, reversal occurs by wall motion; for larger angles, partial rotation occurs, which leaves the film in a partially reversed state with a high stray-field energy. Completion of the reversal takes place, depending on the angle between the field and the easy axis, either by a motion of the walls nucleated at the edges of the film or by the motion of the walls which separate the reversed from the nonreversed bands. The experiments have shown that, except for a field applied in the hard direction, pure uniform rotation as predicted by theory never occurs. For experimental reasons the studies were made on films with a relatively high H_c/H_k ratio. It is believed, however, that this statement is not restricted to the investigated films but applies in general to all Ni-Fe films. In dynamic experiments, as Dietrich[34] has shown, similar partial rotation processes also occur.

Acknowledgment

It is a pleasure to acknowledge the assistance of O. Voegeli, who made the photographs. The author also wishes to thank Dr. E. W. Pugh and Dr. R. E. Matick for valuable discussions.

References

1. M. S. Blois, Jr., *J. Appl. Phys.* **26**, 975 (1955).
2. E. C. Stoner and E. P. Wohlfarth, *Phil. Trans. Roy. Soc. London* **A240**, 599 (1948).
3. J. C. Slonczewski, unpublished work (1956).
4. S. Methfessel, S. Middelhoek, and H. Thomas, *J. Appl. Phys.* **32**, 1959 (1961).
5. D. O. Smith, E. E. Huber, Jr., M. S. Cohen and G. P. Weiss, *J. Appl. Phys.* **31**, 295S (1960).
6. D. O. Smith, *J. Appl. Phys.* **32**, 70S (1961).
7. L. Néel, *J. phys. radium* **17**, 250 (1956).
8. S. Middelhoek, Thesis, University of Amsterdam, 1961.
9. R. E. Behringer and R. S. Smith, *J. Franklin Inst.* **272**, 14 (1961).
10. L. Néel, *Compt. rend.* **241**, 533 (1955).
11. C. O. Tiller and G. W. Clark, *Phys. Rev.* **110**, 583 (1958).
12. J. C. Lloyd and R. S. Smith, *J. Appl. Phys.* **30**, 274S (1959).
13. K. H. Behrndt and F. S. Maddocks, *J. Appl. Phys.* **30**, 276S (1959).
14. S. Methfessel, S. Middelhoek and H. Thomas, *IBM Journal* **4**, 96 (1960).
15. S. Methfessel, A. Segmuller and R. Sommerhalder, *Conference on Magnetism and Crystallographics* Kyoto, Japan, 1961.
16. J. C. Lloyd and R. S. Smith, *Can. J. Phys.* **40**, 454 (1962).
17. I. W. Wolf, *J. Appl. Phys.* **33**, 1152S (1962).
18. E. M. Bradley and M. Prutton, *J. Elec. Control* **6**, 81 (1959).
19. J. B. Goodenough and D. O. Smith, "Magnetic Properties of Thin Films," Ch. 7 in *Magnetic Properties of Metals and Alloys*, American Society for Metals, Cleveland, Ohio, 1959. See p. 140.
20. S. Middelhoek, *Z. angew. Phys.* **13**, 151 (1961).
21. D. O. Smith, *J. Appl. Phys.* **30**, 264S (1959).
22. M. Takahashi, D. Watanabe, T. Kōno and S. Ogawa, *J. Phys. Soc. Japan* **15**, 1351 (1960).
23. M. Prutton and E. M. Bradley, *Proc. Phys. Soc. (London)* **75**, 557 (1960).
24. H. W. Fuller and M. E. Hale, *J. Appl. Phys.* **31**, 238 (1960).
25. E. Fuchs, *Z. angew. Phys.* **13**, 157 (1961).
26. E. Feldtkeller, *Elektron. Rechenanl.* **3**, 167 (1961).
27. S. Middelhoek, *Symposium on the Electric and Magnetic Properties of Thin Metallic Layers*, Leuven, Belgium, 1961.
28. D. O. Smith and K. J. Harte, *J. Appl. Phys.* **33**, 1399 (1962).
29. M. Prutton, *Brit. J. Appl. Phys.* **11**, 335 (1960).
30. H. Thomas, *J. Appl. Phys.* **33**, 1117S (1962).
31. E. H. Frei, S. Shtrikman and D. Treves, *Phys. Rev.* **106**, 446 (1957).
32. S. Middelhoek, *J. Appl. Phys.* **33**, 1111S (1962).
33. E. Feldtkeller, *Symposium on the Electric and Magnetic Properties of Thin Metallic Layers*, Leuven, Belgium, 1961.
34. W. Dietrich, *IBM Journal* **6**, 368 (1962).

Received June 12, 1962